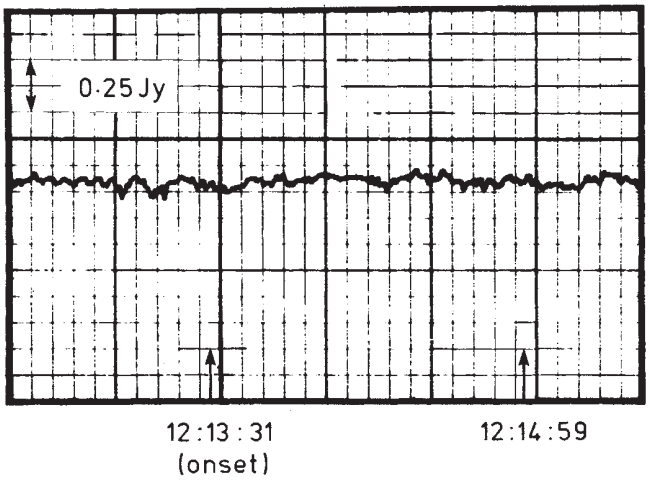

Fig. 1 IR raw data at the K-band corresponding to the time of the X-ray burst, which began at 12 h 13 min 31 s and faded completely into the noise around 12 h 14 min 59 s. The steady level corresponds to the flux from the globular cluster, which has a magnitude of $K = 5.56$ (3.76 Jy) in the 30 arc s aperture.

ponding to the X-ray burst. The steady level corresponds to the flux from the globular cluster. We obtained $K = 5.56$ for the magnitude of the cluster within the 30 arc s aperture, which is consistent with the relation between K-magnitude and aperture size reported by Kleinman *et al.*[8].

The upper limits on variability can be set by using the maximum fluctuations during the observation (times given as UT): $\Delta K < 0.10$ Jy 12 h 13 min 31 s–12 h 14 min 59 s (during the X-ray burst); $\Delta K < 0.25$ Jy 11 h 32 min–12 h 24 min; $\Delta K < 0.4$ Jy 10 h 54 min–11 h 32 min. where 1 Jy corresponds approximately to $K = 7$. Note that the large upper limit of 0.4 Jy in the early part of the observation was probably due to atmospheric conditions and not to luminosity variation of the source.

The upper limit of 0.1 Jy during the type I burst is 70 times smaller than those of reported IR bursts from MXB1730−335. It is unlikely that our time constant of 0.3 s is too long for the detection of IR bursts. Note that Kulkarni *et al.*[4] detected bursts using a time constant of 0.6 s at the H-band as did Jones *et al.*[5] with a time constant of 0.3 s at the K-band.

Our negative result seems to rule out the suggestion by Kulkarni *et al.*[4] that their IR bursts are connected with type I bursts. It is useful to compare our observation with those of other bursters. Coincident X-ray and optical bursts were detected from three type I burst sources, namely 4U/MXB1735−44 (refs 9, 10), MXB1837−05 (ref. 11), and 4U/MXB1636−53 (refs 12, 13). Ten simultaneous X-ray and optical bursts have been observed from 4U/MXB1636−53 by Pedersen *et al.*[12] and Lawrence *et al.*[13] who found that the optical bursts were delayed by a few seconds relative to the X-ray bursts and that the optical burst flux is too large to explain the optical emission as the tail of the black-body X-ray spectrum. It has been suggested[12] that the matter in the vicinity of the X-ray burster absorbs some fractions of the X rays, is heated to $T \sim 50{,}000$ K and re-emits the absorbed energy at optical wavelengths.

The 2.2-μm burst flux which accompanies a type I burst from the rapid burster can be estimated on the assumption that type I bursts from the rapid burster are caused by the same physical process as that suggested for 4U/MXB1636−53; the ratio of the optical peak flux at 3,350–5,250 Å to the bolometric X-ray peak flux is 10^{-3}, after correcting for an interstellar extinction of $A_v = 2.5$ (ref. 11) and assuming that the material heated by the X rays emits a black-body spectrum with $T = 50{,}000$ K at optical and IR wavelengths[13]. The bolometric X-ray burst peak flux of 8×10^{-9} erg s^{-1} cm^{-2} measured by Tenma predicts an apparent 2.2-μm peak flux of 3×10^{-14} erg s^{-1} μm^{-1} cm^{-2} corresponding to 5×10^{-5} Jy assuming an interstellar extinction of $A_K = 1.1$ (ref. 8). This is three orders of magnitude smaller than our upper limit of 0.1 Jy during the type I burst. Hence, if a fraction of type I bursts are accompanied by the reported IR bursts, the mechanism should be quite different from that suggested to explain the well known optical bursts of normal bursters. We note that Lewin *et al.*[14] have also reported the absence of an IR burst during a type I X-ray burst from Ser X-1.

Jones *et al.*[5] pointed out that neither type I nor type II bursts fit the reported IR bursts, whose pattern of occurrence differs from those of X-ray bursts. We conclude that type I bursts do not seem to be accompanied by the reported IR bursts. However, we cannot rule out the possibility that a fraction of type I bursts may be accompanied by the reported IR bursts, as we have only observed one type I burst which shows no IR counterpart.

We thank Dr H. Kunieda and his collaborators from Nagoya University and the Institute of Space and Astronautical Science for providing X-ray data before publication and for collaboration. We also thank Professor H. Okuda for useful suggestions and correspondence.

Received 1 March; accepted 30 April 1984.

1. Lewin, W. H. G. *et al. Astrophys. J. Lett.* **207**, L95–L99 (1976).
2. Liller, W. *Astrophys. J. Lett.* **213**, L21–L23 (1977).
3. Lawrence, A. *et al. Astrophys. J.* **267**, 301–309 (1983).
4. Kulkarni, P. V., Ashok, N. M., Apparao, K. M. V. & Chitre S. M. *Nature* **280**, 819–820 (1979).
5. Jones, A. W. *et al. Nature* **283**, 550–551 (1980).
6. Sato, S., Kawara, K., Kobayashi, Y., Maihara, T. & Okuda, H. *Nature* **286**, 688–689 (1980).
7. Kunieda, H. *et al.* Preprint, Nagoya Univ. (1984).
8. Kleinmann, D. E., Kleinmann, S. G. & Wright, E. L. *Astrophys. J. Lett.* **210**, L83–L86 (1976).
9. Grindlay, J. E. *et al. Nature* 274, 567–568 (1978).
10. McClintock, J. E. *et al. Nature* **279**, 47–49 (1979).
11. Hackwell, J. A. *et al. Astrophys. J. Lett.* **223**, L115–L119 (1979).
12. Pedersen, H. *et al. Astrophys. J.* **263**, 325–339 (1982).
13. Lawrence, A. *et al. Astrophys. J.* **271**, 793–803 (1983).
14. Lewin, W. H. G. *et al. Nature* **287**, 27–28 (1980).

First optical detection of atomic deuterium in the upper atmosphere from Spacelab 1

J. L. Bertaux*, F. Goutail*, E. Dimarellis*, G. Kockarts† & E. Van Ransbeeck†

*Service d'Aéronomie du CNRS, BP 3, F-91370 Verrières-le-Buisson, France
† Institut d'Aéronomie Spatiale, 3 Avenue Circulaire, B-1180 Bruxelles, Belgium

Measurements of the deuterium-to-hydrogen ratios (D/H) in the fields of meteorology[1,2], tropospheric[3,4] and stratospheric chemistry[5,6], planetology[7,8] and cosmogony[8,9] have previously been performed on molecules in which one hydrogen atom is replaced by one deuterium atom. We report here the first detection of isolated deuterium atoms in the Earth's upper atmosphere through their resonantly scattered Lyman-α emission. An atmospheric deuterium emission of 330 R ($1\ R = 10^6$ photons cm^{-2} s^{-1}) is observed for a tangent altitude of 110 km during Spacelab 1 mission launched on 28 November 1983. The (D/H) ratio of 3×10^{-4} is slightly enriched over the seawater value of 1.6×10^{-4}.

In the terrestrial upper atmosphere, hydrogen atoms are illuminated by the intense solar Lyα line at the resonance wavelength of 121.566 nm in the far UV. The solar Lyα is so wide that it can also illuminate deuterium atoms at the resonance wavelength of 121.533 nm. Through resonant scattering, hydrogen and deuterium can re-emit their Lyα line. Although hydrogen Lyα emission has been observed many times from space, deuterium Lyα has not been detected for two reasons. First, the (D/H) ratio in seawater is only 1.6×10^{-4}. Second, the spectral distance between the two Lyα lines is quite small.

However, the resonance lines of both isotopes are well separated, as their spectral distance of 0.033 nm is much larger than their thermal width of ~0.002 nm. Consequently, the spectral

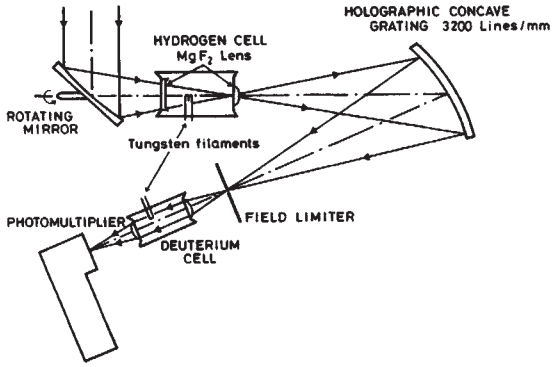

Fig. 1 Optical diagram of experiment 1ES017. The mass of the instrument is 12.5 kg. The dimensions are 685 × 300 × 320 mm and the average power required is 30 W.

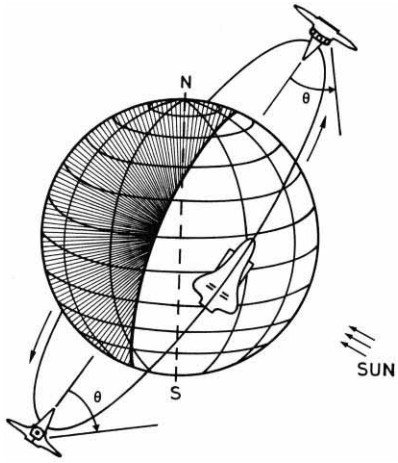

Fig. 2 Geometrical configuration for bright limb observations from an altitude of 250 km. The orbit altitude sketch is greatly exaggerated in respect to the Earth's radius.

resolution needed to distinguish them would have meant using a prohibitively large and heavy classical spectrometer on this first Spacelab mission. We have, therefore, designed and built a lightweight spectrophotometer (Fig. 1) equipped with molecular hydrogen and deuterium absorption cells to suppress selectively one or two of the natural emissions of both isotopes H and D recorded by the instrument. Atmospheric light is collected with a small parabolic off-axis mirror, rotating around one axis to provide a vertical scan of the emission around the limb. The light goes through the hydrogen cell, which is transparent to Lyα when it is not activated, and enters a spectrometer with a single concave holographic grating. A hole at the exit defines both the 2.5° circular field of view of the instrument and a spectral bandwidth of ~4.5 nm centred at Lyα. Thus, the strong atmospheric emission line of atomic oxygen at 130.4 nm is eliminated. The light is then focused on the photomultiplier window through the deuterium cell equipped with MgF_2 lenses. Photons are counted in two counters, sequentially opened in phase with a 5-Hz modulation of the deuterium cell: one counter C_1 is devoted to photons when the deuterium cell is off, the other counter C_2 is devoted to photons when the deuterium cell is activated, that is, when molecular deuterium is dissociated into atoms in the cell.

Fortunately, the atomic hydrogen Lyα emission is saturated, when looking towards the limb, because of the large H column density in the line-of-sight, whereas the optically thin emission I_D of D atoms is proportional to the D column density. As a result, the intensity ratio I_D/I_H is much larger than the (D/H) ratio.

The geometry of observations is illustrated in Fig. 2. The limb is observed from an altitude of 250 km at right angles to the orbital plane, in order to cancel the Doppler shift associated with the 8 km s^{-1} space shuttle velocity. Otherwise, the absorption cells would have had little or no effect on the atmospheric H and D emissions.

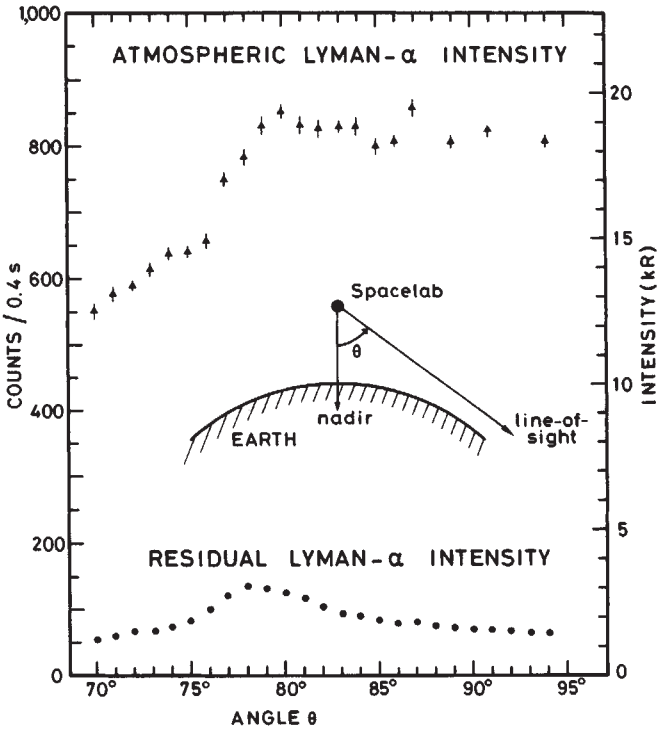

Fig. 3 Measured atmospheric Lyα intensity is shown in the upper part. The residual Lyα intensity indicated in the lower part corresponds to the intensity which is not absorbed when the hydrogen cell is turned on. The left-hand ordinate corresponds to the photomultiplier count rate which is converted into kR in the right-hand scale. The geometrical significance of the observational angle θ is shown in the centre.

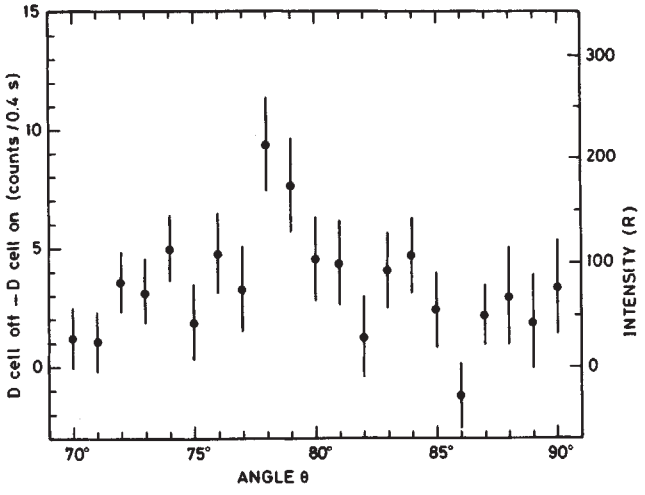

Fig. 4 Atmospheric deuterium Lyα intensity absorbed by the activated deuterium cell. During these measurements the hydrogen cell is permanently on whereas the deuterium cell is alternatively switched on and off. The measured points represent an average of 74 angle scans. Angle θ has the same significance as in Fig. 3.

The measured intensity, which essentially results from H Lyα emission, is displayed in the upper part of Fig. 3 as a function of the angle θ with the local vertical. When approaching the limb from below, the H Lyα increases up to the point where the line-of-sight passes above 110 km altitude, corresponding to $\theta = 78°$. Above this height, absorption of Lyα emission by atmospheric molecular oxygen becomes negligible and the Lyα intensity reaches 20 kR.

When a tungsten ribbon is heated electrically in the H_2 cell, an optical thickness $\tau_H \cong 600$ of atomic H is created inside the cell, which absorbs a large fraction (80–90%) of the total signal. The H_2 cell acts as a 'negative' filter and lets through every photon with a wavelength lying outside the absorption profile, which has an equivalent width of 0.006 nm. The transmitted signal is recorded by counter C_1 and shown at the bottom of Fig. 3. It contains mainly H Lyα photons from the linewings, which extend slightly outside the negative filter because of saturation effects.

A small contribution of atmospheric deuterium Lyα emission can then be identified by using the deuterium cell, which creates an optical thickness $\tau_D \cong 1.5$, representing a negative filter selective for D Lyα emission. For $\tau_D = 1.5$, it can be shown that ~60% of the deuterium intensity I_D is absorbed in the cell, and the difference between the two counters $C_1 - C_2$ represents a measurement of $0.6 I_D$. This absorbed intensity is plotted both in counts per 0.4 s and in Rayleighs in Fig. 4.

Seventy-four scans around the limb were averaged and binned in steps of $\Delta\theta = 1°$ to obtain the curve in Fig. 4, representing ~100 min of measurements spread over three orbits and a large range of latitudes. The size of the error bar attached to $C_1 - C_2$ is 2.5 times the error bar attached to counts C_1, which is $(C_1/n)^{1/2}$. Without measurable deuterium emission I_D, the points would be equally positive or negative, which is not the case. Except for one value at $\theta = 86°$, all points are positive, which means that atmospheric deuterium Lyα emission has been unambiguously detected.

A narrow maximum of deuterium emission is found around $\theta = 78°$, at an altitude of ~110 km. This limb brightening effect is expected from the optically thin deuterium emission, when the line-of-sight passes just above the Lyα limb created by atmospheric O_2 absorption. As the field of view of the instrument is 2.5°, it means that the observable deuterium layer is even smaller than what is shown in Fig. 4. However, we can produce a preliminary estimate of the deuterium quantity corresponding to our observations. Because the emitted deuterium Lyα intensity I_D is 330 R, the column number density N_D and the intensity I_D are linked by:

$$I_D(\mathrm{R}) = 10^{-6} \sigma F_s N_D = 10^{-6}\, g\, N_D$$

where F_s is the solar flux[10] of 2.8×10^{12} photons cm^{-2} s^{-1} nm^{-1}. Because the integrated cross-section of D atoms is $\sigma = 5.43 \times 10^{-16}$ cm^2 nm, the excitation rate of D atoms by solar photons is $g = \sigma F_s = 1.52 \times 10^{-3}$ s^{-1}, and these photons are scattered isotropically.

For $I_D = 330$ R, $N_D = 2.2 \times 10^{11}$ atoms cm^{-2} along the line-of-sight tangent at 110-km altitude. We have compared this integrated density to a vertical distribution model depending mainly on one parameter, the eddy diffusion coefficient K, which indicates roughly the altitude of the homopause level, where the atmosphere goes from a well mixed regime to one in which all gases are distributed according to their own scale height and mass. It has been shown[11] that the (D/H) ratio is sensitive to this value of K and also to the exospheric temperature T. Our value of $N_D = 2.2 \times 10^{11}$ atoms cm^{-2} corresponds to a model with a thermopause temperature of 900 K in which the number density is 2.5×10^3 cm^{-3} at 110 km of altitude, and the (D/H) ratio is of the order of 3×10^{-4}. This modest enrichment by a factor of 2 corresponds to a height-independent eddy diffusion coefficient of 1.3×10^6 cm^2 s^{-1}.

Our deuterium observations were hampered during this Spacelab mission by two problems. First, the sensitivity of our first flight model was a factor of 4 below its nominal value, while a second unit unfortunately achieved nominal sensitivity too late to be accommodated in the Spacelab payload. Second, the orbit, because of date and time of launch, soon shifted towards a position near the terminator, where excitation of deuterium atoms by solar Lyα photons is decreased by a larger O_2 column density. As a result, we could observe deuterium emission only during the first 24 h, although the mission lasted for 10 days. A second mission could help to establish a variation of the homopause level with latitude, a major atmospheric objective.

Nevertheless, we have demonstrated that the natural Lyα emission of deuterium atoms can be used to evaluate their number density in the Earth's atmosphere by a remote-sensing technique.

Finally, this remote-sensing technique could be used with the Space Telescope or space probes for the other planets, in particular for Venus and Mars, where the (D/H) ratio is unknown. For Venus, a (D/H) ratio of 1.6×10^{-2} was found[7] in a cloud droplet sucked by a neutral mass spectrometer on board the large probe of Pioneer Venus mission. Such a high value can be explained only by a fantastic differential escape of both isotopes[12,13], the heavier D atoms being left behind in the atmosphere of Venus. The quantity of water at the origin of Venus was at least 100 times larger[7] than it is now.

Such an important clue about the history of water on Venus deserves further investigation. We have demonstrated the feasibility of the deuterium Lyα detection technique. It can now be applied to detailed terrestrial and planetary studies.

We acknowledge the financial support of the French Centre National d'Etudes Spatiales (CNES) and of the Belgian Administration de la Recherche Scientifique (Ministry of National Education). The technical support of ESA and NASA during integration and flight was greatly appreciated.

Received 8 March; accepted 26 April 1984.

1. Lawrence, J. R., Gedzelman, S. D., White, J. W. C., Smiley, D. & Lazov, P. *Nature* **296**, 638–640 (1982).
2. Leguy, C., Rindsberger, M., Zangwil, A., Issar, A. & Gat, J. R. *Isot. Geosci.* **1**, 205–218 (1983).
3. Ehhalt, D., Roether, W. & Stich, W. *Z. Naturforsch.* **21a**, 1703–1709 (1966).
4. Ehhalt, D. & Ostlund, H. G. *J. geophys. Res.* **75**, 2323–2327 (1970).
5. Scholz, T. G., Ehhalt, D. H., Heidt, L. E. & Martell, E. A. *J. geophys. Res.* **75**, 3049–3054 (1970).
6. Pollock, W., Heidt, L. E., Lueb, R. & Ehhalt, D. H. *J. geophys. Res.* **85**, 5555–5568 (1980).
7. Donahue, T. M., Hoffman, J. H., Hodges, R. R. Jr & Watson, A. H. *Science* **216**, 630–633 (1982).
8. Gautier, D. & Owen, T. *Nature* **304**, 691–694 (1983).
9. Geiss, J. & Reeves, H. *Astr. Astrophys.* **93**, 189–199 (1981).
10. Lemaire, P. *et al. Astrophys. J. Lett.* **223**, L55–L58 (1978).
11. Kockarts, G. *Space Res.* **12**, 1047–1050 (1972).
12. Kasting, J. F. & Pollack, J. B. *Icarus* **53**, 479–508 (1983).
13. Kumar, S., Hunten, D. M. & Pollack, J. B. *Icarus* **55**, 369–383 (1983).

Crustal evolution in north-east and east Africa from model Nd ages

N. B. W. Harris, C. J. Hawkesworth & A. C. Ries

Department of Earth Sciences, The Open University, Milton Keynes MK7 6AA, UK

The relationships between the various crustal provinces that comprise north-east and east Africa are far from clear and reflect diverse tectonic and magmatic processes which took place during the Proterozoic. Here we present the results of an Nd isotope study on the major rock units of the Pan-African (1,100–500 Myr BP) terrane. Charnockites from Jabel Uweinat, a basement inlier at the junction of Egypt, Libya and the Sudan, yield middle Archaean model Nd ages, whilst model ages of <1,200 Myr have been obtained in a belt from the Eastern Desert of Egypt to north-west Kenya. This, therefore, represents a westward extension of the juvenile Pan-African crust of the Arabian Shield (Fig. 1). The shield itself is characterized by comparatively rapid crustal growth[1], probably in an accreting island arc environment[2]. Between the two areas, there is a marginal zone of Pan-African rocks with relatively low $\varepsilon_{Nd}(T)$ values (see Table 1) due to increased contributions from the pre-Pan African crust. Overall, the Pan-African rocks from north-east and east Africa and those from the Damara of Namibia[3] exhibit a wide range of $\varepsilon_{Nd}(T)$ from +7.5 to −18.0 which reflects regional changes in tectonic style and is not readily reconciled with simple models for the evolution of average continental crust.